ACS APPLIED BIO MATERIALS

www.acsabm.org Article

Design of a Thiol-Responsive, Traceless Prodrug with Rapid Self-Immolation for Cancer Chemotherapy

Gengqi Liu,[‖] Zhen Jiang,[‖] Jonathan F. Lovell, Lei Zhang, and Yumiao Zhang*

Cite This: https://doi.org/10.1021/acsabm.1c00247 Read Online

ACCESS | Metrics & More | Article Recommendations | Supporting Information

ABSTRACT: Prodrugs can be formed by chemical modification of the existing active pharmaceutical ingredients (APIs); however, this often sacrifices their functional efficacy. Self-immolative linkers have recently attracted attention, as they can be designed to release pristine APIs. Herein, we report a strategy to generate a self-immolative prodrug (SIP) that can release pristine doxorubicin (DOX). Compared to conventional linkers, the key SIP DOX (KSIP-DOX) developed here can rapidly and quantitatively release the API due to its strong leaving group after reduction by thiol groups, which are present in tumors. KSIP-DOX has enhanced cellular uptake and improved anticancer efficacy, demonstrating its utility for cancer treatment.

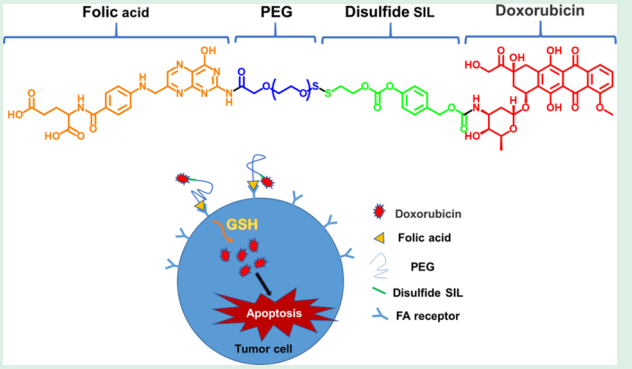

KEYWORDS: *self-immolation, cross-linker, doxorubicin, antitumor, drug release*

1. INTRODUCTION

Various prodrug strategies were designed for the development of new anticancer prodrugs responsive to external stimuli including redox,[1,2] pH,[3−5] and other stimuli.[6−8] Conventional cross-linkers involve direct conjugation of active pharmaceutical ingredients (APIs) to the triggering group, which changes the chemical structure of the APIs for prolonged periods and which has therapeutic effects.[9,10] Self-immolative linkers (SILs), composed of a reactive site, a self-immolation spacer, and a stimuli responsive moiety, have gained attention, as they can release pristine APIs under external stimuli conditions in a controlled fashion.[11−13] Two main classes of reduction-sensitive linkers have been used for this purpose; disulfide carbamates[14,15] and dithiobenzyl carbamates.[16−18] Reduction-sensitive SILs operate on the significant difference in glutathione (GSH) concentration. For example, tumor cells have a higher GSH concentration than normal cells.[19] Also, the concentration of intracellular GSH (1−10 mM) is about 3 orders of magnitude higher than the concentration of GSH in serum.[20] Thus, SILs are minimally cleaved in serum while circulating but are cleaved to release anticancer drugs in tumor cells. In spite of their potential, their applications for drug delivery are still limited by their slow self-immolation rate or incomplete release of pristine drugs. Therefore, new SILs that can reversibly modify drugs and rapidly release them in a traceless manner would be of interest.

Doxorubicin (DOX) is a widely used cancer chemotherapy drug. Various DOX prodrugs and nanoparticles have been developed to enhance the anticancer effect of DOX.[21,22] Yet, many of these methods fail to guarantee the complete and fast drug release, so that the side groups left on the APIs after crack in the disulfide bond reduce its bioactivity.[10,16,23,24] In addition, for active-targeted delivery of DOX, folic acid (FA) has been commonly used as a targeting moiety for the testing of targeted agents. The folate receptor has a high affinity and specificity for FA and its derivatives such as methyl tetrahydrofolate.[25,26] The expression level of FA receptors on some tumor cells is much higher than that of normal cells.[27,28]

Considering these aforementioned points, we herein design a new DOX prodrug composed of four moieties: (1) DOX as the API, (2) FA as a targeting moiety, (3) (ethylene glycol) (PEG) to increase water solubility, and (4) a novel "key SIL" to rapidly release DOX. As control, a self-immolative drug of DOX was designed with the same scheme but using a conventional benzyl carbamate-based linker instead. The two DOX prodrugs synthesized by a key linker and control linker are termed as a key self-immolative prodrug (KSIP-DOX) and control SIP (CSIP-DOX). KSIP-DOX can release DOX within minutes in the presence of GSH found in cancer cells. It also has good water solubility, better targeting capability, and longer circulation time in blood. Owing to the SIL design, KSIP-DOX can rapidly and quantitatively release DOX

Received: February 25, 2021
Accepted: May 11, 2021

without chemical modification with a half-life of about 20 min after cleavage by 10 mM GSH, whereas CSIP-DOX exhibits a much slower release rate of pristine drugs. Compared with free DOX and CSIP-DOX, KSIP-DOX is better uptaken by cancer cells and shows enhanced efficacy against tumor cells.

2. EXPERIMENTAL SECTION

2.1. Synthesis of Thiol-Responsive Self-Immolative Cross-linkers and Drug Conjugates. See Supporting Information.

2.2. Cleavage Kinetics of DOX Conjugates. 100 μL of compound 9 or compound 10 (5 μmol/mL) in DMSO was added to 90 μL of 10 mM GSH in water. The centrifuge tube was placed in a 37 °C incubator, incubated for different times, and then sampled for the analysis with HPLC, monitoring the absorption at 480 nm. The elution buffer was performed with A: H_2O and B: acetonitrile (0.1% trifluoroacetic acid). The gradient used was 0−5 min, 30−40% B; 5−10 min, 40−50% B; 10−20 min, 50−60% B; and 20−30 min, 60−70% B for the linker-DOX cleavage, peaks representing free DOX and linker DOX were integrated, and the percentage of free DOX released was calculated as the $area^{DOX}/area^{DOX}$.

2.3. Characterization of KSIP-DOX. Fluorescence spectra and the UV−vis absorbance spectrum of KSIP-DOX were measured by a microplate reader (Tecan infinite 200). Zetasizer was used to detect the size and particle size distributions of KSIP-DOX. The samples were diluted in water and analyzed (n = 3). To test the stability of KSIP-DOX in different media, samples were diluted in water, PBS, or FBS (10%) and size was recorded using the Zetasizer (n = 3).

2.4. *In Vitro* Drug Release. PBS (30 mL, with 1% Tween 80, pH = 7.4) with or without 10 mM GSH was prepared and added into a 50 mL centrifuge tube. Then, 1 mL of KSIP-DOX and CSIP-DOX in the prepared phosphate buffer saline (PBS, with or without 10 mM GSH) was put in a dialysis bag (molecular weight cut: 2000 D). At the predetermined time points, 100 μL of the solution was removed from the tube outside the dialysis bag, and 100 μL of the corresponding fresh PBS (with or without 10 mM GSH) was supplemented. Then, the DOX fluorescence intensity in the removed solution was analyzed with a microplate reader (λ_{ex} = 480 nm, λ_{em} = 596 nm).

2.5. Cell and Animal Studies. Mouse melanoma cells: B16 cell lines were kindly provided from Prof. Shaokai Sun's group from school of medical imaging, Tianjin Medical University, Tianjin.

Six week old female Balb/c nude mice (20 ± 2 g) and eight week old CD-1 mice were purchased from Charles River Beijing Co., Ltd (Beijing, China). Mice were maintained and treated according to the US National Institutes of Health policy on laboratory animal care and use guidelines, and the protocols were approved by Tianjin University Institutional Animal Care and Use Committee (Protocol number: TJUE-2020-034).

The *in vitro* cytotoxicity of the KSIP-DOX prodrug and free drugs was examined using the CCK-8 assay. B16 cells were transferred to 96-well plates (5000 cells per well) and incubated for 24 h, and then, the original medium was replaced with fresh medium with KSIP-DOX, CSIP-DOX, KSIP-DOX-F^-, and free DOX in different concentrations (1, 2, or 5 μg/mL). In addition, B16 cells were transferred to a 96-well plate (5000 cells per well) and incubated for 24 h. Then, the original medium was replaced with fresh medium with KSIP-DOX, CSIP-DOX, KSIP-DOX-F^-, and free DOX (1 μg/mL), and it was incubated for different times (4, 8, or 12 h). Then, the CCK-8 reagent (100 μL/mL) was added to each well and incubated at 37 °C for 1 h in a cell culture incubator. The absorbance of each well was measured at 450 nm.

2.6. Cellular Uptake and Distribution. B16 cells were transferred to a 24-well plate at a density of 5×10^4 cells per well and incubated at 37 °C for 24 h. Then, the previous medium was replaced with 500 μL fresh medium containing KSIP-DOX, CSIP-DOX, KSIP-DOX-F^-, and free DOX (5 μg/mL) and then further incubated for different times (0.5, 1, 2, 4, and 12 h). Untreated cells served as control. Finally, we used PBS to wash each well, and B16 cells were decomposed with TX-100 solution (1%). Then, each well was analyzed for the intracellular fluorescence by using a microplate reader. For fluorescence imaging, B16 cells were transferred to confocal dish (1×10^5 cells per well) and cultured for 24 h. After incubation, the previous medium was replaced with 1 mL fresh medium containing KSIP-DOX, CSIP-DOX, KSIP-DOX-F^-, and free DOX (DOX concentration: 5 μg/mL) and then was further incubated for 4 h. Then, each dish was washed two times with PBS, and paraformaldehyde was used to fix cells. After rinsing with PBS two times, we stained the cells with DAPI (1 μg/mL) for 5 min. Fluorescence images of treated cells were acquired under a laser scanning confocal microscope.

2.7. *In Vivo* Pharmacokinetics and Biodistribution Study. CD-1 mice of the same age were divided into three groups at random (KSIP-DOX group, CSIP-DOX, free DOX injection group). Each group was injected with different DOX formulations (5 mg/kg) through the tail vein. Then, we collected blood samples at different time points (0.5, 1, 2, 4, 8, and 24 h), placed them at 4 °C for 1 h, and centrifuged at 1000g for 10 min at 4 °C to separate plasma.

Then, we prepared plasma samples for analysis, used methyl-4-hydroxybenzoate as an internal standard, and added 100 μL of serum, 50 μL of methyl-4-hydroxybenzoate (1 μg/mL), and 600 μL of acetonitrile to the centrifuge tube. Then, we vortexed the centrifuge tube containing the mixture for 3 min. After centrifugation at 4000g for 10 min, the supernatant (700 μL) was collected. The solvent was evaporated under vacuum and redissolved with 100 μL of mobile phase buffer before the HPLC measurement.

The mobile phase was composed of methanol, acetonitrile (0.1% TFA), and Milli-Q water (23:17:60 v/v). The peak monitoring wavelength was 240 nm. 20 μL of the sample solution was injected, and the flow rate was 1 mL/min for analysis.

For the biodistribution study, three CD-1 mice of the same age and similar body weight were selected at random. Each mouse was injected into the tail vein and received different DOX formulations (10 mg/kg). The organs of different mice were placed in 1.5 mL of PBS and homogenized at a high speed for 3 min using a homogenizer. After centrifugation at 4000g for 10 min in 4 °C, 1 mL of the supernatant was collected in a test tube, and then, we added 50 μL of methyl-4-hydroxybenzoate (1 μg/mL) and 600 μL of acetonitrile in a centrifuge tube. We vortexed the centrifuge tube containing the mixture for 3 min. The supernatant (500 μL) was collected after centrifugation at 4000g for 10 min at 4 °C. The solvent was evaporated under vacuum and redissolved with 100 μL of mobile phase buffer before the HPLC measurement.

2.8. Toxicity Evaluation *In Vivo*. For the evaluation of nephrotoxicity and hepatotoxicity of KSIP-DOX, mice were divided into PBS and KSIP-DOX groups (5 mg/kg, n = 3). All mice were given PBS or drugs intravenously three times (on day 1, 3, and 5), and the body weight was weighed and recorded every day. Then, we collected blood samples on the day 8 and used them for further toxicity analysis.

To determine the nephrotoxicity caused by KSIP-DOX, the blood was centrifuged at 1000g for 10 min at 4 °C and analyzed using biochemical assay kits [NGAL (neutrophil gelatinase-associated lipocalin) and BUN (blood urea nitrogen)].

To determine the hepatotoxicity caused by KSIP-DOX, the blood was centrifuged at 1000g for 10 min at 4 °C and analyzed using biochemical assay kits [AST (aspartate aminotransferase), ALT (alanine aminotransferase), and AKP (alkaline phosphatase)].

2.9. *In Vivo* Anticancer Efficacy. B16 cells (100 μL, containing 5×10^7 cells) were injected into the subcutaneous area of the right back of nude mice to establish a tumor-bearing mouse model. When the tumor volume of the mice increased to about 100 mm^3, we divided the tumor-bearing mice into five groups (n = 3) at random, and (1) free DOX, (2) KSIP-DOX, (3) CSIP-DOX, (4) KSIP-DOX-F^-, and (5) normal saline were injected through the tail vein on day 1, 3, and 5 until the end of the treatment on day 7. The dose of DOX is 5 mg/kg. We monitored and recorded the tumor volume and body weight of mice every day.

$$\text{tumor volume} = (\text{longest diameter} \times \text{shortest diameter}^2)/2$$

https://doi.org/10.1021/acsabm.1c00247
ACS Appl. Bio Mater. XXXX, XXX, XXX−XXX

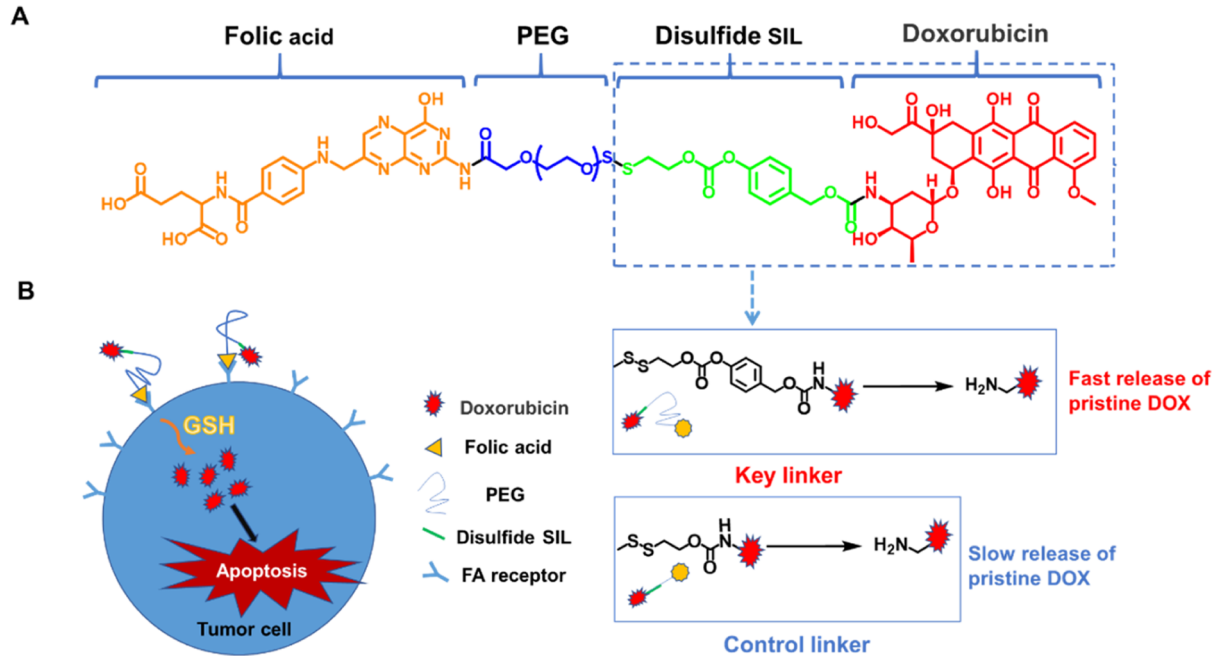

Figure 1. (A) Structure of the key SIP DOX, KSIP-DOX. (B) Schematic illustration of KSIP-DOX-mediated chemotherapy after its disulfide bond is cleaved by GSH in tumor cells, releasing free DOX in a fast manner, compared to CSIP-DOX replacing the self-immolative key linker with the control linker.

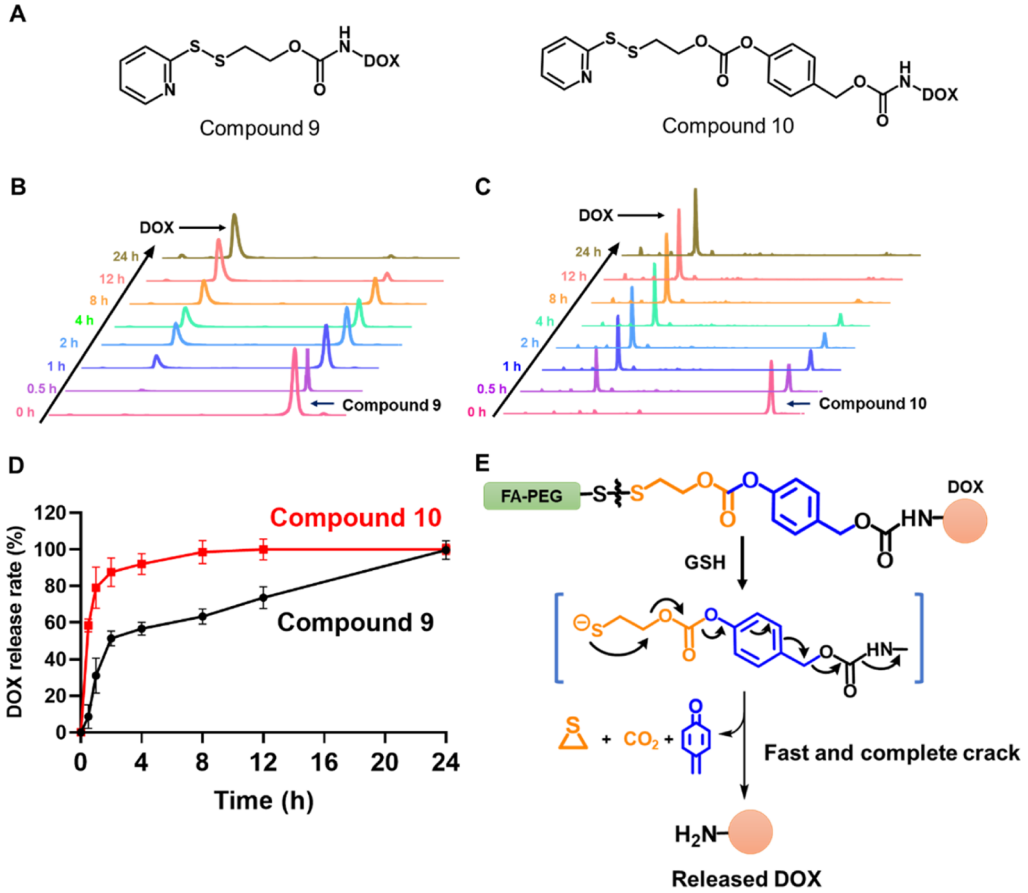

Figure 2. Fast self-immolation rate of compound 10 (A) chemical structures of compounds 9 and 10 for the analysis of self-immolation kinetics. HPLC analysis for DOX that is released from (B) compound 9 (5 μmol/mL) and (C) compound 10 (5 μmol/mL) in a system containing 10 mM GSH as a thiol trigger. (D) DOX-released percentage from compound 9 and compound 10 in a system containing 10 mM GSH. (E) Scheme for the self-immolation mechanism of KSIP-DOX.

https://doi.org/10.1021/acsabm.1c00247
ACS Appl. Bio Mater. XXXX, XXX, XXX−XXX

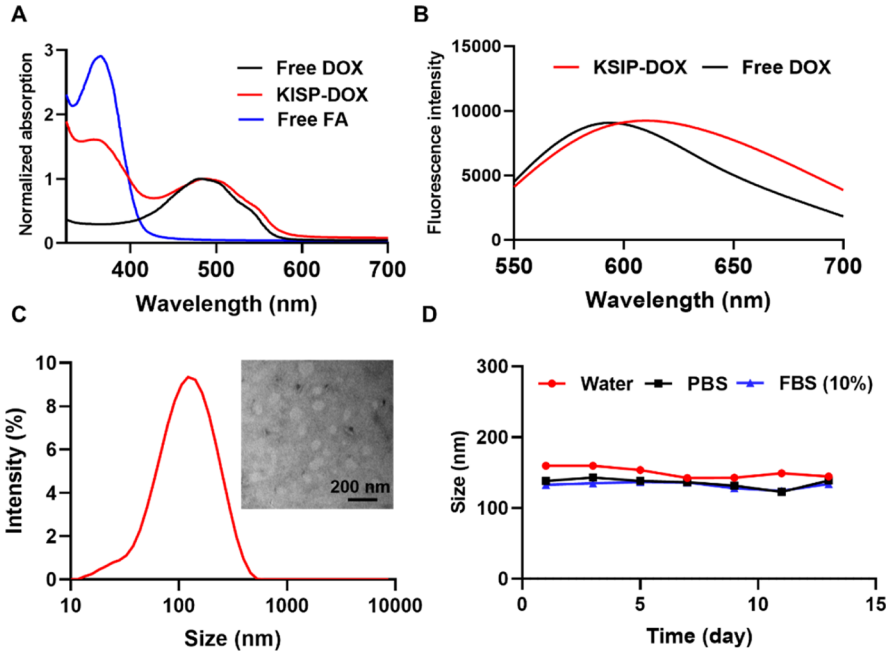

Figure 3. (A) Absorbance spectrum of free aqueous DOX, folate, and KSIP-DOX conjugates. (B) Fluorescence spectrum of aqueous KSIP-DOX and free DOX. (C) DLS of KSIP-DOX in water solution and TEM images. (D) Stability of KSIP-DOX in different media (Water, PBS, and 10% FBS) for 13 days.

3. RESULTS AND DISCUSSION

As shown in Figure 1, KSIP-DOX was designed with three moieties including the key SIL, PEG, and FA conjugated in series connected to the amines of DOX. Responsive to reducing thiols in tumor cells, the disulfide SIL can release pristine DOX without chemical pedants left on the API. PEG and FA moieties offer functionalities of improved solubility and targeting, respectively. In comparison with free DOX and CSIP-DOX, KSIP-DOX can specifically target tumor cells and rapidly release DOX. In order to achieve the traceless release free DOX, we designed two SILs with different decomposition rates, key SIL (compound 8) and control SIL (compound 5). Also, the synthetic route of the two cross-linkers is shown in Figure S1A, and the synthetic route of their corresponding DOX prodrugs, termed as KSIP-DOX and CSIP-DOX, is shown in Figure S1B. The intermediate and final products were characterized by ^{1}H NMR, ^{13}C NMR, and HR/MS (Figures S2−S27)

Next, we investigated the cleavage kinetics of the self-immolative moieties of these two DOX prodrugs. The DOX-conjugated key cross-linker (compound 10) and DOX-conjugated control cross-linker (compound 9) without FA and PEG moieties were chosen for this comparison in the presence of 10 mM GSH (the chemical structures of compound 9 and compound 10 and their synthetic routes are shown in Figures 2A and S1C). Compound 9 or 10 was dissolved in DMSO, mixed with aqueous GSH, and then subjected to HPLC analysis at different time points. As demonstrated in Figure 2B,C, being responsive to 10 mM GSH, both compounds 9 and 10 were hydrolyzed and released free DOX, indicated by the DOX peaks monitored by HPLC at 480 nm. However, the key cross-linker exhibited a faster rate of self-immolation, and the half-life of the DOX release was 20 min. By contrast, the control cross-linker did not release completely until 24 h (Figure 2D). A similar trend was also shown in aqueous medium (Figure S28). Previously, we have shown that the newly designed cross-linker with thiol-ethyl carbonate and 1,6-elimination spacers can completely release amine-containing drugs in a faster mode, whereas the conventional cross-linkers for amine modification such as the dithiobenzyl carbamates and disulfide carbamates cannot.[29] After disulfide reduction, the key cross-linker undergoes the cyclization of free thiol and 1,6-elimination, eventually releasing the primary amine on DOX. Two self-immolation mechanisms of such a type of linker after the reduction of the disulfide bond were previously reported including the elimination of the five-membered ring 1,3-oxathiolan-2-one or the elimination of the three-membered ring of thiirane and carbon dioxide.[30−32] The latter one involving the generation of the three-membered ring 1,3-oxathiolan-2-one is more likely to occur, although some studies also proposed the simultaneity of these two scenarios;[33,34] so, the mechanism of self-immolation for the key cross-linker in this work was proposed, as shown in Figure 2E.

As shown in Figure 3A, KSIP-DOX has characteristic absorption maxima at wavelengths at 480 and 365 nm, indicative of the presence of DOX or FA. The fluorescence spectrum showed that KSIP-DOX had an emission wavelength maximum around 600 nm, exhibiting a slight red shift compared to free DOX with emission maxima at about 595 nm (Figure 3B) because the addition of PEG and linker structures to the prodrug altered the optical property of DOX. Because KSIP-DOX has amphiphilic blocks, KSIP-DOX self-assembled into nanoparticles around 100 nm characterized by transmission electron microscopy (TEM) and dynamic light scattering (DLS). In addition, the size of KSIP-DOX remained almost the same in different solutions including water, PBS, or 10% FBS medium within a time course around 2 weeks (Figure 3D).

Then, we investigated the pharmacokinetics of KSIP-DOX on mice. As shown in Figure 4A, after mice were intravenously administered KSIP-DOX, CSIP-DOX, or free DOX (5 mg/kg

https://doi.org/10.1021/acsabm.1c00247
ACS Appl. Bio Mater. XXXX, XXX, XXX−XXX

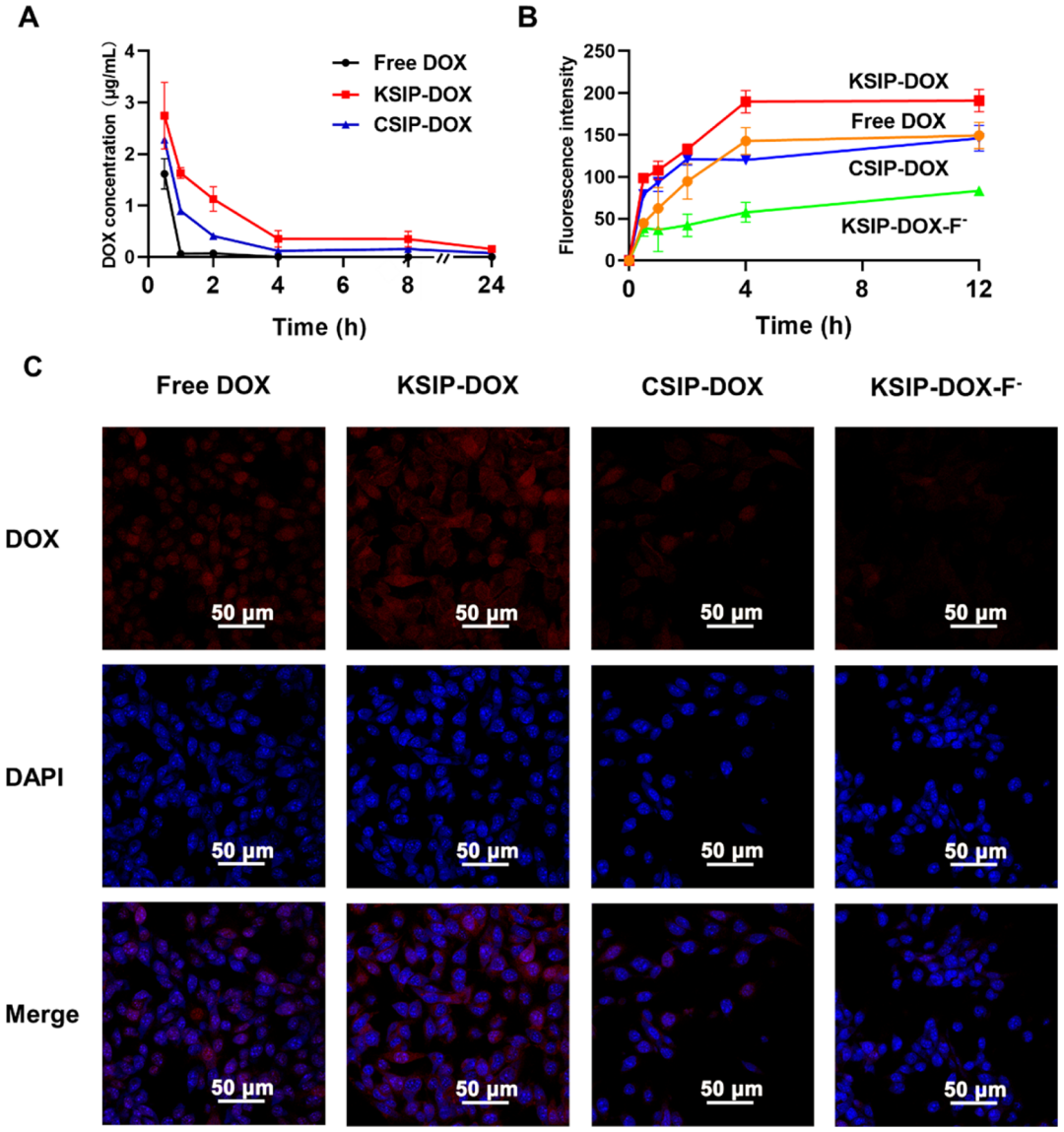

Figure 4. (A) Pharmacokinetics of KSIP-DOX, CSIP-DOX, and free DOX in mice. DOX concentration was measured by HPLC after mice were intravenously administered KSIP-DOX, CSIP-DOX, or free DOX (5 mg/kg DOX), and the blood was collected after 24 h. B16 cells were incubated with KSIP-DOX, CSIP-DOX, free DOX, and KSIP-DOX-F$^-$ for 4 h, followed by cell lysis by TX-100, and then, the cellular uptake was quantified by measuring (B) fluorescence of DOX; and (C) laser scanning confocal microscopy images.

DOX), the peak DOX concentration (C_{max}) of the KSIP-DOX group (2.75 μg/mL) was higher than that of the free DOX (1.61 μg/mL) group or CSIP-DOX (2.27 μg/mL). Also, the serum half-life in the KSIP-DOX group (5.81 h) was also longer than that in the free DOX group (1.4 h) or CSIP-DOX (4.78 h). These results indicated that DOX in the form of KSIP-DOX exhibited prolonged blood circulation time. Next, we assessed the DOX uptake and distribution in B16 tumor cells when treated with various DOX formulations including free DOX, KSIP-DOX, CSIP-DOX, and KSIP-DOX without folate (KSIP-DOX-F$^-$) under different treatment conditions. As shown in Figure 4B, KSIP-DOX had the highest cellular uptake efficiency and the uptake was saturated around 4 h, whereas KSIP-DOX-F$^-$ had the lowest cellular uptake efficiency. The enhanced cellular uptake was ascribed to the targeting of FA expressed on B16 tumor cells or possibly enhanced phagocytosis. Furthermore, we also investigated the cell uptake by laser scanning confocal microscopy after B16 tumor cells were treated with different DOX formulations for 4 h. As demonstrated in Figure 4C, the DOX fluorescence intensity (red) of KSIP-DOX was significantly higher than other groups, which is consistent with the data of the cellular uptake shown in Figure 4B. The observed nuclear localization is expected for liberated DOX. These results indicate that when DOX exists in the form of KSIP-DOX, it will enhance the uptake of DOX by tumor cells. In comparison with CSIP-DOX, the higher cellular uptake of KSIP-DOX is probably ascribed to the more hydrophobic moiety, and previously, it was also shown that hydrophobic modification of drugs can facilitate translocation across the membrane and phagocytosis.[35−37]

Encouraged by the improved cellular uptake, we next evaluated antitumor efficacy of KSIP-DOX. First, the efficacy of KSIP-DOX was assessed on the B16 cell line using the CCK-8 viability assay. As shown in Figure 5A, the cell viability decreased as DOX concentration increased after incubation

https://doi.org/10.1021/acsabm.1c00247
ACS Appl. Bio Mater. XXXX, XXX, XXX−XXX

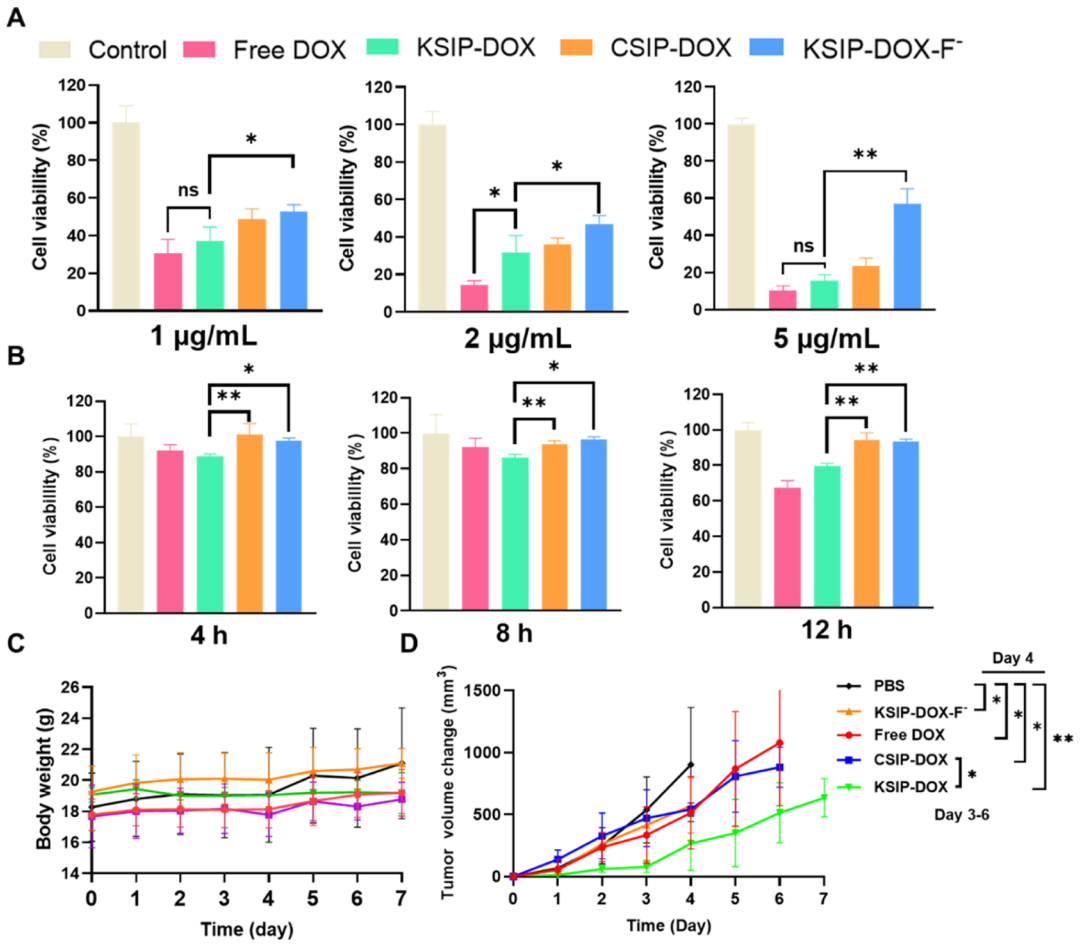

Figure 5. Antitumor effects of KSIP-DOX. (A) B16 cell viability after incubation with different DOX concentrations of KSIP-DOX, CSIP-DOX, free DOX, and KSIP-DOX-F⁻ (1, 2, and 5 μg/mL) for 24 h. (B) B16 Cell viability after incubation with KSIP-DOX, CSIP-DOX, free DOX, and KSIP-DOX-F⁻ (1 μg/mL DOX) for different times (4, 8, and 12 h). *In vivo* antitumor efficacy of KSIP-DOX. The (C) body weight and (D) tumor size change of B16 tumor-bearing mice treated with PBS, KSIP-DOX, CSIP-DOX, free DOX, or KSIP-DOX-F⁻. (One-way analysis of variance was used for significant difference analysis, ns $P > 0.05$, *$P < 0.05$, **$P < 0.01$).

with different DOX formulations for 24 h including free DOX, KSIP-DOX, CSIP-DOX, and KSIP-DOX-F⁻, showing a dose-dependent cytotoxicity. Among these groups, the cytotoxicity of KSIP-DOX was almost the same as that of the free DOX group. KSIP-DOX exhibited more cytotoxicity than CSIP-DOX and KSIP-DOX-F⁻ groups. As shown in Figure 5B, the KSIP-DOX group had higher cytotoxicity than other prodrug treatments after incubation with B16 cells for 4, 8, or 12 h, and it also had cytotoxicity similar to the DOX group. This can be explained by the fact that KSIP-DOX can rapidly release DOX for the effective antitumor effect. Next, the efficacy of KSIP-DOX was evaluated *in vivo*. Bearing-tumor nude mice were intravenously administered PBS or 5 mg/kg DOX of free DOX, KSIP-DOX, CSIP-DOX, or KSIP-DOX-F⁻. Then, we monitored the body weight and tumor size every day. As demonstrated in Figure 5C, no obvious body weight loss occurred, suggesting that these formulations had no noticeable toxicity at these doses, at least within the time window of 1 week. As demonstrated in Figure 5D, compared to the PBS group, the CSIP-DOX group showed a significant difference in inhibition of tumor growth. In comparison with other groups, the KSIP-DOX group has a significant inhibitory effect on tumor growth.

Previously, it was demonstrated that the wide application of DOX is limited by its nephrotoxicity and hepatotoxicity,[38−40] and we found that KSIP-DOX primarily accumulated in liver, as shown in Figure S29; so, we further assessed the toxicity of KSIP-DOX *in vivo* including nephrotoxicity and hepatotoxicity when mice were treated by the same treatment scheme shown in Figure 5. BUN and NGAL are two biomarkers used to assess nephrotoxicity.[41] As shown in Figure S30A,B, the level of NGAL and BUN has no significant difference when mice were given PBS or 5 mg/kg (DOX) KSIP-DOX three times for 7 days. Then, we also assessed the AST, ALT, and AKP in serum, which are biomarkers of the liver function. As shown in Figure S30C−E, the PBS group and KSIP-DOX group show no significant difference in the level of AST, ALT, and AKP. These results indicate that KSIP-DOX presents a safe prodrug for cancer chemotherapy.

4. CONCLUSIONS

In conclusion, we developed a thiol-responsive and traceless antitumor prodrug with rapid self-immolation. Compared with traditional SILs, the KSIL can quantitively and rapidly release pristine amine-containing drugs. KSIP-DOX has longer circulation times in serum and enhanced cell uptake in tumor cells owing to the chemistry design in the KSIL including the good leaving group and fast self-immolation rate. KSIP-DOX with better solubility, targeting capability, and

https://doi.org/10.1021/acsabm.1c00247
ACS Appl. Bio Mater. XXXX, XXX, XXX−XXX

enhanced antitumor efficacy represents a new and enabling prodrug, showing its promise for cancer treatment.

■ ASSOCIATED CONTENT

Supporting Information

The Supporting Information is available free of charge at https://pubs.acs.org/doi/10.1021/acsabm.1c00247.

Synthesis of thiol-responsive self-immolative crosslinkers and drug conjugates; ^{1}H NMR spectra, ^{13}C NMR spectra; HR/MS spectra; *in vitro* release profiles; biodistribution; and *in vivo* toxicity evaluation (PDF)

■ AUTHOR INFORMATION

Corresponding Author

Yumiao Zhang − *School of Chemical Engineering and Technology, Tianjin University, Tianjin 300350, China; Key Laboratory of Systems Bioengineering (Ministry of Education), Tianjin University, Tianjin 300350, P. R. China;* orcid.org/0000-0002-6166-0470; Email: ymzhang88@tju.edu.cn

Authors

Gengqi Liu − *School of Chemical Engineering and Technology, Tianjin University, Tianjin 300350, China; Key Laboratory of Systems Bioengineering (Ministry of Education), Tianjin University, Tianjin 300350, P. R. China*

Zhen Jiang − *School of Chemical Engineering and Technology, Tianjin University, Tianjin 300350, China; Key Laboratory of Systems Bioengineering (Ministry of Education), Tianjin University, Tianjin 300350, P. R. China*

Jonathan F. Lovell − *Department of Biomedical Engineering, The State University of New York at Buffalo, Buffalo, New York 14260, United States;* orcid.org/0000-0002-9052-884X

Lei Zhang − *School of Chemical Engineering and Technology, Tianjin University, Tianjin 300350, China; Key Laboratory of Systems Bioengineering (Ministry of Education), Tianjin University, Tianjin 300350, P. R. China;* orcid.org/0000-0003-3638-6219

Complete contact information is available at: https://pubs.acs.org/10.1021/acsabm.1c00247

Author Contributions

‖G.L. and Z.J. authors contributed equally.

Funding

This work is supported by the Start-Up grant at Tianjin University (Y.Z.) and One-Thousand Young Talent Program (Y.Z.) and the National Natural Science Foundation of China (32071384 to Y.Z.).

Notes

The authors declare no competing financial interest.

■ REFERENCES

(1) Lu, B.; Xiao, F.; Wang, Z.; Wang, B.; Pan, Z.; Zhao, W.; Zhu, Z.; Zhang, J. Redox-Sensitive Hyaluronic Acid Polymer Prodrug Nanoparticles for Enhancing Intracellular Drug Self-Delivery and Targeted Cancer Therapy. *ACS Biomater. Sci. Eng.* **2020**, *6*, 4106−4115.

(2) Zhang, F.; Zhu, G.; Jacobson, O.; Liu, Y.; Chen, K.; Yu, G.; Ni, Q.; Fan, J.; Yang, Z.; Xu, F.; Fu, X.; Wang, Z.; Ma, Y.; Niu, G.; Zhao, X.; Chen, X. Transformative Nanomedicine of an Amphiphilic Camptothecin Prodrug for Long Circulation and High Tumor Uptake in Cancer Therapy. *ACS Nano* **2017**, *11*, 8838−8848.

(3) Dong, S.; Sun, Y.; Liu, J.; Li, L.; He, J.; Zhang, M.; Ni, P. Multifunctional Polymeric Prodrug with Simultaneous Conjugating Camptothecin and Doxorubicin for pH/Reduction Dual-Responsive Drug Delivery. *ACS Appl. Mater. Interfaces* **2019**, *11*, 8740−8748.

(4) Li, L.; Li, D.; Zhang, M.; He, J.; Liu, J.; Ni, P. One-Pot Synthesis of pH/Redox Responsive Polymeric Prodrug and Fabrication of Shell Cross-Linked Prodrug Micelles for Antitumor Drug Transportation. *Bioconjugate Chem.* **2018**, *29*, 2806−2817.

(5) Reinhard, S.; Han, H.; Tuma, J.; Røise, J. J.; Li, I.-C.; Li, J.; Lee, H. Y.; Murthy, N. A pH-sensitive eosin-block copolymer delivers proteins intracellularly. *Chem. Commun.* **2020**, *56*, 14207−14210.

(6) Li, J.; Cui, D.; Huang, J.; He, S.; Pu, K. Organic Semiconducting Pro-nanostimulants for Near-Infrared Photoactivatable Cancer Immunotherapy. *Angew. Chem., Int. Ed.* **2019**, *58*, 12680.

(7) Phua, S. Z. F.; Xue, C.; Lim, W. Q.; Yang, G.; Chen, H.; Zhang, Y.; Wijaya, C. F.; Luo, Z.; Zhao, Y. Light-Responsive Prodrug-Based Supramolecular Nanosystems for Site-Specific Combination Therapy of Cancer. *Chem. Mater.* **2019**, *31*, 3349−3358.

(8) Dai, L.; Cai, R.; Li, M.; Luo, Z.; Yu, Y.; Chen, W.; Shen, X.; Pei, Y.; Zhao, X.; Cai, K. Dual-Targeted Cascade-Responsive Prodrug Micelle System for Tumor Therapy in Vivo. *Chem. Mater.* **2017**, *29*, 6976−6992.

(9) Böhme, D.; Beck-Sickinger, A. G. Drug delivery and release systems for targeted tumor therapy. *J. Pept. Sci.* **2015**, *21*, 186−200.

(10) Chen, J.; Zhao, M.; Feng, F.; Sizovs, A.; Wang, J. Tunable Thioesters as "Reduction" Responsive Functionality for Traceless Reversible Protein PEGylation. *J. Am. Chem. Soc.* **2013**, *135*, 10938−10941.

(11) Rautio, J.; Kumpulainen, H.; Heimbach, T.; Oliyai, R.; Oh, D.; Järvinen, T.; Savolainen, J. Prodrugs: Design and clinical applications. *Nat. Rev. Drug Discovery* **2008**, *7*, 255−270.

(12) Kratz, F.; Müller, I. A.; Ryppa, C.; Warnecke, A. Prodrug Strategies in Anticancer Chemotherapy. *ChemMedChem* **2010**, *3*, 20−53.

(13) Bildstein, L.; Dubernet, C.; Couvreur, P. Prodrug-based intracellular delivery of anticancer agents. *Adv. Drug Delivery Rev.* **2011**, *63*, 3−23.

(14) Zhang, H.; Wang, K.; Na, K.; Li, D.; Li, Z.; Zhao, D.; Zhong, L.; Wang, M.; Kou, L.; Luo, C.; Zhang, H.; Kan, Q.; Ding, H.; He, Z.; Sun, J. Striking a Balance between Carbonate/Carbamate Linkage Bond- and Reduction-Sensitive Disulfide Bond-Bearing Linker for Tailored Controlled Release: In Situ Covalent-Albumin-Binding Gemcitabine Prodrugs Promote Bioavailability and Tumor Accumulation. *J. Med. Chem.* **2018**, *61*, 4904−4917.

(15) Zhang, X.; Zhang, M.; Wang, M.; Peng, H.; Hua, Q.; Ma, L.; Wang, B.; Wei, H. Facile Fabrication of 10-Hydroxycamptothecin-Backboned Amphiphilic Polyprodrug with Precisely Tailored Drug Loading Content for Controlled Release. *Bioconjugate Chem.* **2018**, *29*, 2239−2247.

(16) Zalipsky, S.; Mullah, N.; Engbers, C.; Hutchins, M. U.; Kiwan, R. Thiolytically Cleavable Dithiobenzyl Urethane-Linked Polymer−Protein Conjugates as Macromolecular Prodrugs: Reversible PEGylation of Proteins. *Bioconjugate Chem.* **2007**, *18*, 1869−1878.

(17) Zalipsky, S.; Qazen, M.; Walker, J. A.; Mullah, N.; Quinn, Y. P.; Huang, S. K. New Detachable Poly(ethylene glycol) Conjugates: Cysteine-Cleavable Lipopolymers Regenerating Natural Phospholipid, Diacyl Phosphatidylethanolamine. *Bioconjugate Chem.* **1999**, *10*, 703−707.

(18) Senter, P. D.; Pearce, W. E.; Greenfield, R. S. Development of a drug-release strategy based on the reductive fragmentation of benzyl carbamate disulfides. *J. Org. Chem.* **1990**, *55*, 2975−2978.

(19) Kuppusamy, P.; Li, H.; Ilangovan, G.; Cardounel, A. J.; Zweier, J. L.; Yamada, K.; Krishna, M. C.; Mitchell, J. B. Noninvasive imaging of tumor redox status and its modification by tissue glutathione levels. *Cancer Res.* **2002**, *62*, 307.

(20) Wu, G.; Fang, Y.-Z.; Yang, S.; Lupton, J. R.; Turner, N. D. Glutathione Metabolism and Its Implications for Health. *J. Nutr.* **2004**, *134*, 489−492.

(21) Li, S.; Jiang, X.; Zheng, R.; Zuo, S.; Zhao, L.; Fan, G.; Fan, J.; Liao, Y.; Yu, X.; Cheng, H. An azobenzene-based heteromeric prodrug for hypoxia-activated chemotherapy by regulating subcellular localization. *Chem. Commun.* **2018**, *54*, 7983−7986.
(22) Kiran, S.; Dwivedi, P.; Khatik, R.; Hameed, S.; Dwivedi, M.; Huang, F.; Xu, R. X. Synthesis of a functionalized dipeptide for targeted delivery and pH-sensitive release of chemotherapeutics. *Chem. Commun.* **2020**, *56*, 285−288.
(23) Shechter, Y.; Mironchik, M.; Saul, A.; Gershonov, E.; Precido-Patt, L.; Sasson, K.; Tsubery, H.; Mester, B.; Kapitkovsky, A.; Rubinraut, S.; Vachutinski, Y.; Fridkin, G.; Fridkin, M. New Technologies to Prolong Life-time of Peptide and Protein Drugs In vivo. *Int. J. Pept. Res. Ther.* **2007**, *13*, 105−117.
(24) Gong, Y.; Leroux, J.-C.; Gauthier, M. A. Releasable Conjugation of Polymers to Proteins. *Bioconjugate Chem.* **2015**, *26*, 1172−1181.
(25) Low, P. S.; Henne, W. A.; Doorneweerd, D. D. Discovery and Development of Folic-Acid-Based Receptor Targeting for Imaging and Therapy of Cancer and Inflammatory Diseases. *Acc. Chem. Res.* **2008**, *41*, 120−129.
(26) Chen, C.; Ke, J.; Zhou, X. E.; Yi, W.; Brunzelle, J. S.; Li, J.; Yong, E.-L.; Xu, H. E.; Melcher, K. Structural basis for molecular recognition of folic acid by folate receptors. *Nature* **2013**, *500*, 486−489.
(27) Kelemen, L. E. The role of folate receptor α in cancer development, progression and treatment: Cause, consequence or innocent bystander? *Int. J. Cancer* **2006**, *119*, 243−250.
(28) Kane, M. A.; Elwood, P. C.; Portillo, R. M.; Antony, A. C.; Najfeld, V.; Finley, A.; Waxman, S.; Kolhouse, J. F. Influence on immunoreactive folate-binding proteins of extracellular folate concentration in cultured human cells. *J. Clin. Invest.* **1988**, *81*, 1398−1406.
(29) He, M.; Li, J.; Han, H.; Borges, C. A.; Neiman, G.; Røise, J. J.; Hadaczek, P.; Mendonsa, R.; Holm, V. R.; Wilson, R. C.; Bankiewicz, K.; Zhang, Y.; Sadlowski, C. M.; Healy, K.; Riley, L. W.; Murthy, N. A traceless linker for aliphatic amines that rapidly and quantitatively fragments after reduction. *Chem. Sci.* **2020**, *11*, 8973−8980.
(30) Batisse, C.; Dransart, E.; Ait Sarkouh, R.; Brulle, L.; Bai, S.-K.; Godefroy, S.; Johannes, L.; Schmidt, F. A new delivery system for auristatin in STxB-drug conjugate therapy. *Eur. J. Med. Chem.* **2015**, *95*, 483−491.
(31) Jones, L. R.; Goun, E. A.; Shinde, R.; Rothbard, J. B.; Contag, C. H.; Wender, P. A. Releasable Luciferin−Transporter Conjugates: Tools for the Real-Time Analysis of Cellular Uptake and Release. *J. Am. Chem. Soc.* **2006**, *128*, 6526−6527.
(32) Deng, Z.; Hu, J.; Liu, S. Disulfide-Based Self-Immolative Linkers and Functional Bioconjugates for Biological Applications. *Macromol. Rapid Commun.* **2020**, *41*, 1900531.
(33) Jain, A. K.; Gund, M. G.; Desai, D. C.; Borhade, N.; Senthilkumar, S. P.; Dhiman, M.; Mangu, N. K.; Mali, S. V.; Dubash, N. P.; Halder, S.; Satyam, A. Mutual prodrugs containing bio-cleavable and drug releasable disulfide linkers. *Bioorg. Chem.* **2013**, *49*, 40−48.
(34) Satyam, A. Design and synthesis of releasable folate−drug conjugates using a novel heterobifunctional disulfide-containing linker. *Bioorg. Med. Chem. Lett.* **2008**, *18*, 3196−3199.
(35) Sakagami, K.; Masuda, T.; Kawano, K.; Futaki, S. Importance of Net Hydrophobicity in the Cellular Uptake of All-Hydrocarbon Stapled Peptides. *Mol. Pharm.* **2018**, *15*, 1332−1340.
(36) Missirlis, D.; Khant, H.; Tirrell, M. Mechanisms of Peptide Amphiphile Internalization by SJSA-1 Cells in Vitro. *Biochemistry* **2009**, *48*, 3304−3314.
(37) van Rijt, S. H.; Mukherjee, A.; Pizarro, A. M.; Sadler, P. J. Cytotoxicity, Hydrophobicity, Uptake, and Distribution of Osmium-(II) Anticancer Complexes in Ovarian Cancer Cells. *J. Med. Chem.* **2010**, *53*, 840−849.
(38) Sinha, B. K.; Katki, A. G.; Batist, G.; Cowan, K. H.; Myers, C. E. Adriamycin-stimulated hydroxyl radical formation in human breast tumor cells. *Biochem. Pharmacol.* **1987**, *36*, 793−796.
(39) Herman, E. H.; Zhang, J.; Chadwick, D. P.; Ferrans, V. J. Comparison of the protective effects of amifostine and dexrazoxane against the toxicity of doxorubicin in spontaneously hypertensive rats. *Cancer Chemother. Pharmacol.* **2000**, *45*, 329−334.
(40) Saad, S. Y.; Najjar, T. A.; Al-Rikabi, A. C. The preventive role of deferoxamine against acute doxorubicin-induced cardiac, renal and hepatic toxicity in rats. *Pharmacol. Res.* **2001**, *43*, 211−218.
(41) Yang, X.; Ren, H.; Zhang, H.; Liu, G.; Jiang, Z.; Qiu, Q.; Yu, C.; Murthy, N.; Zhao, K.; Lovell, J. F.; Zhang, Y. Antibiotic Cross-linked Micelles with Reduced Toxicity for Multidrug-Resistant Bacterial Sepsis Treatment. *ACS Appl. Mater. Interfaces* **2021**, *13*, 9630−9642.

https://doi.org/10.1021/acsabm.1c00247
ACS Appl. Bio Mater. XXXX, XXX, XXX−XXX